ACADEMIC PRESS

Available online at www.sciencedirect.com

SCIENCE DIRECT®

Molecular Phylogenetics and Evolution 26 (2003) 389–408

MOLECULAR PHYLOGENETICS AND EVOLUTION

www.elsevier.com/locate/ympev

Extensive mtDNA variation within the yellow-pine chipmunk, *Tamias amoenus* (Rodentia: Sciuridae), and phylogeographic inferences for northwest North America

John R. Demboski* and Jack Sullivan

Department of Biological Sciences, University of Idaho, P.O. Box 443051, Moscow, ID 83844-3051, USA

Received 2 August 2001; received in revised form 2 July 2002

Abstract

The yellow-pine chipmunk, *Tamias amoenus*, is common in xerophytic forests throughout much of northwest North America. We analyzed cytochrome *b* sequence variation from 155 individuals representing 57 localities across the distribution of *T. amoenus* including 10 additional species of *Tamias*. Maximum likelihood and parsimony tree estimation methods were used in conjunction with nested clade analysis to infer both deep and population-level processes. Our results indicate that two currently recognized subspecies of *T. amoenus* (*T. a. canicaudus* and *T. a. cratericus*) are not nested within other samples of *T. amoenus*. Maximum uncorrected levels of intraspecific sequence divergence within remaining samples of *T. amoenus* are >7%. Substantial geographic variation is characterized by 12 well-supported clades that correspond to distinct mountain ranges, but do not necessarily follow existing subspecific taxonomy. Significant association between geography and genealogy was detected within many of these clades and can be attributed to different population-level processes including past fragmentation, recent range expansion, and isolation by distance.

Keywords: Cytochrome *b*; Likelihood; Nested clade analysis; Phylogeny

1. Introduction

Unraveling the phylogeographic history of a species is dependent upon an understanding of both the contemporary and historical processes that have shaped underlying genetic structure relative to geography. Deeper historical effects may be the result of past climatic or geological events that have promoted singular or episodic events of vicariance leading to subsequent diversification (Webb and Bartlein, 1992). Shallow, more contemporary, processes may include the effects of post-glacial range expansion and retraction leading to secondary contact between differentiated lineages (Hewitt, 1996; Templeton, 1998). Given the observation that many phylogeographic studies are characterized by both deep and shallow history (Riddle, 1996), it is critical to employ analytical approaches that can provide resolution of these related, but temporally separated events.

Tree-building methods, such as parsimony or maximum likelihood, have been commonly used in phylogeographic studies (Avise, 2000). However, intraspecific data sets are often characterized by well-supported clades that consist of a large number of nearly identical haplotypes. In these cases, these approaches may provide only limited resolution of intraclade relationships since the small number of substitutions that differentiate non-bifurcating haplotypes result in multiple, equally optimal solutions. Network methods based on coalescent theory (e.g., nested clade analysis; Templeton et al., 1987) have been used to tease apart these shallow "tip" relationships and allow rigorous inference of processes affecting genealogical and geographic structure at the population level (summarized in Posada and Crandall, 2001). When tree-estimation and network methods are

* Corresponding author. Present address: Biological Sciences Department, California State Polytechnic University, Pomona, 3801 West Temple Ave., Pomona, CA 91768-4032, USA. Fax: 1-909-869-4078.

E-mail address: jrdemboski@csupomona.edu (J.R. Demboski).

1055-7903/02/$ - see front matter © 2002 Elsevier Science (USA). All rights reserved.
doi:10.1016/S1055-7903(02)00363-9

used in conjunction, they provide a rigorous analytical framework with which to address biogeographic questions (Nielson et al., 2001).

Molecular phylogeographic studies have contributed a great deal to our understanding of the biogeographic history of western North America (Brunsfeld et al., 2001; Cook et al., 2001; Soltis et al., 1997; Zink, 1996). Within mammals, identification of otherwise cryptic lineages suggests, as Riddle and Hafner (1999) have stressed, that characterization of the evolutionary and biogeographic history of North American mammals is far from complete. Large-scale phylogeographic patterns, such as the North Pacific Coastal/Continental dichotomy, have been uncovered by the comparison of multiple species (Cook et al., 2001). The origin of this deep bifurcation most likely predates the Late Pleistocene (Arbogast, 1999), and in many cases current taxonomy does not reflect this molecular dichotomy (Cook and MacDonald, 2001). One hypothesis erected to explain this common phylogeographic pattern is that it is a result of concerted responses of taxa and boreal forest communities to climatic fluctuations initiated during the Early to Mid Pleistocene (Arbogast, 1999). However, forests in western North America are heterogeneous composites that include very distinct mesic and xerophytic communities (Baker, 1983; Daubenmire, 1975), and the phylogeographic histories of many species are likely tied to the patchy, ephemeral nature of these forest communities. For more restricted taxa found in western North America, additional biogeographic hypotheses have also been erected (summarized in Brunsfeld et al., 2001).

One group of mammals suggested to have diversified in response to climatic events and subsequent habitat shifts is the chipmunk genus *Tamias* (Hoffmann, 1981). *Tamias* includes 25 species of small, diurnal squirrels with most of the diversity centered in western North America (23 species; Hoffmann et al., 1993). Species or species groups within *Tamias* are tied to distinct habitats (Johnson, 1943), and serve as textbook examples of interspecific niche partitioning (Hoffmann, 1981). In western North America, the second most widely distributed species is the yellow-pine chipmunk (*Tamias amoenus*). Its distribution encompasses the northern Rocky Mountains, Cascade Range, and numerous peripheral mountain ranges such as the Sierra Nevada Mountains and central Oregon Highlands (Fig. 1). Throughout its range, the yellow-pine chipmunk is common in xerophytic forests characterized by open stands of ponderosa pine (*Pinus ponderosa*) and Douglas-fir (*Pseudotsuga menziesii*; Sutton, 1992). The patchy distribution of this habitat provides the opportunity for substantial geographic subdivision within *T. amoenus*. For example, the Columbia Basin effectively bisects the central part of its distribution, resulting in large regions of discontinuous habitat (Fig. 1). Where mesic and xeric habitats are interspersed in the Cascade Range, northern Rocky Mountains, and Sierra Nevada Range, *T. amoenus* is sympatric (but not necessarily syntopic) with other species of *Tamias* (Sutton, 1992).

Two studies examining phylogenetic relationships based on morphological, allozyme, and molecular data sets have concluded that *T. amoenus* is monophyletic (Levenson et al., 1985; Piaggio and Spicer, 2001). However, its position within *Tamias* has remained unclear and it has been placed in various species groups (Allen, 1891; Howell, 1929; Levenson et al., 1985; Piaggio and Spicer, 2000; White, 1953). Within *T. amoenus*, 14 morphological subspecies have been recognized (Fig. 1; Sutton, 1992). Levenson et al. (1985) noted intraspecific differences in allele frequencies among four subspecies of *T. amoenus*, including the presence of three rare alleles in the eastern subspecies, *T. a. luteiventris*. This is in line with Piaggio and Spicer (2001) who observed intraspecific variation (~3% uncorrected) within the mitochondrial cytochrome *b* (cyt *b*) gene among four populations sampled from California, Washington and Wyoming.

In this study, we use a combination of tree-estimation and nested clade methodologies to infer both deep and more contemporary phylogeographic processes from a large cyt *b* data set ($n = 165$). Our analyses expand on previous studies that included *T. amoenus* but were focused on resolving interspecific relationships within *Tamias* (Levenson et al., 1985; Piaggio and Spicer, 2001). The broad geographic and sampling breadth of this study provides new insights regarding the systematics and phylogeography of the yellow-pine chipmunk.

2. Materials and methods

2.1. Specimens examined

We examined 155 specimens of *T. amoenus* from 57 sampling localities (Appendix A; Fig. 1). We attempted to sample *T. amoenus* throughout its range and collected multiple individuals from 36 localities. Seventy-one chipmunks were collected during fieldwork conducted between 1999 and 2000. Additional samples were obtained by loans of tissue or museum skin samples from various sources (Appendix A). Except where noted, specimens were prepared as standard museum study skins or skeletons (with the baculum cleared and stained) and deposited in the University of Idaho Vertebrate Collection. We also included five cyt *b* sequences of *T. amoenus* from Piaggio and Spicer (2001). Given the large uncorrected sequence divergence among individuals currently assigned to *T. amoenus* (8.9%; see below) and the lack of unambiguous sister species for *T. amoenus* (Piaggio and Spicer, 2000), additional samples representing species groups defined by Piaggio and

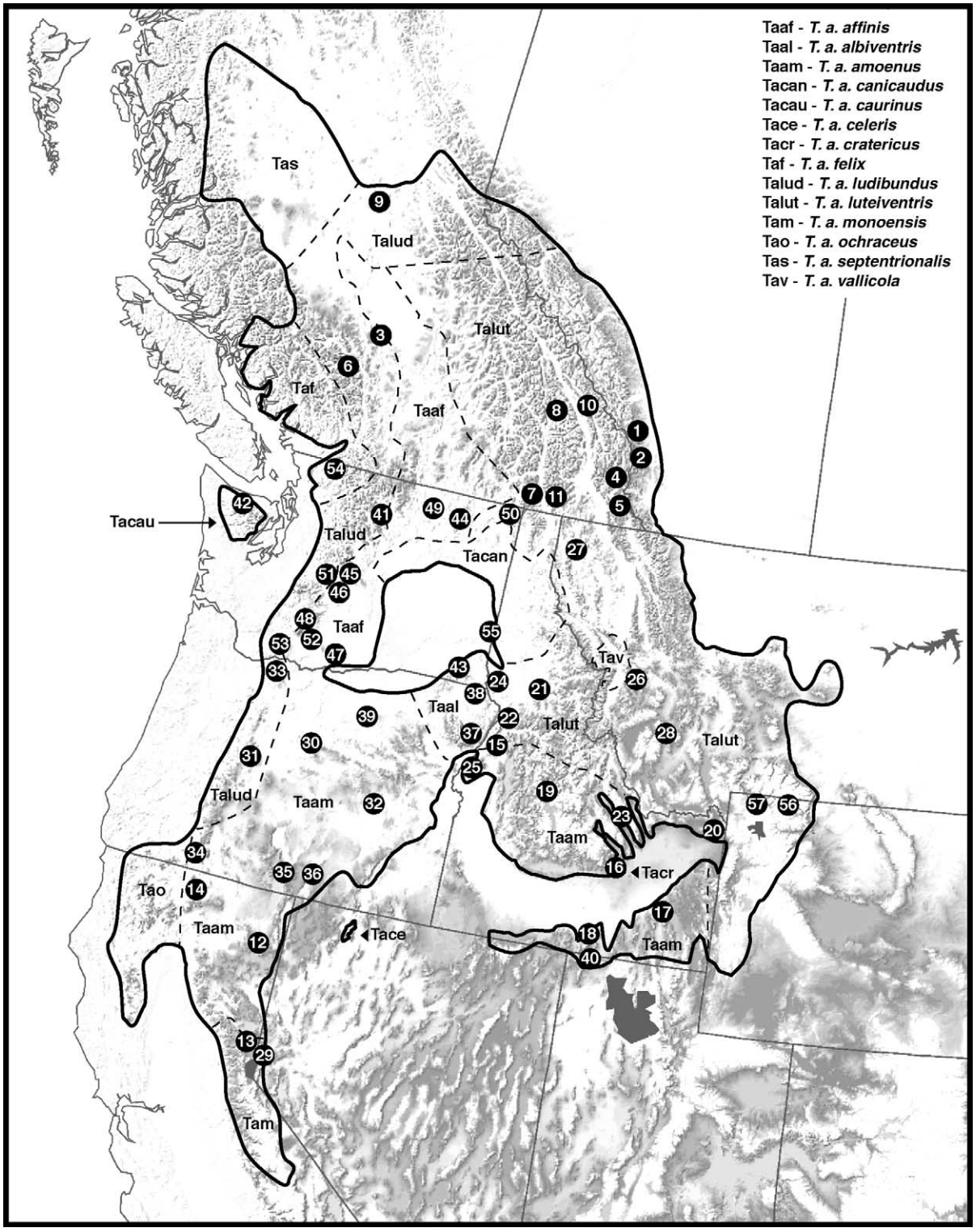

Fig. 1. Map of western North America depicting *T. amoenus* sample sites described in the Appendix A. The distribution of *T. amoenus* (solid lines) was modified from Hall (1981) and Verts and Carraway (1998). Subspecific boundaries are depicted with dashed lines.

Spicer (2000) were included. These included *T. dorsalis* and *T. quadrivittatus* (*T. quadrivittatus* group), *T. merriami* (*T. merriami* group), *T. minimus* and *T. ruficaudus* (*T. minimus* group), *T. senex*, *T. siskiyou*, and *T. townsendii* (*T. townsendii* group), and an additional species not examined by Piaggio and Spicer (2000), *T. speciosus*. Our sampling was designed to include representatives of these species that are found in sympatry with *T. amoenus. Tamias sibiricus*, often assigned to the separate genus or subgenus, *Eutamias* (Levenson et al.,

1985; Piaggio and Spicer, 2000) was the designated outgroup for all phylogenetic analyses. The complete data set consisted of 165 individuals.

2.2. DNA isolation, amplification, sequencing, and alignment

Total genomic DNA was extracted from tissue samples using a DTAB/CTAB protocol modified from Gustincich et al. (1991). In addition, genomic DNA was extracted from 17 museum study skins with the Qiagen DNeasy Tissue Kit using the rodent tail protocol. Skin extractions and PCR amplifications were conducted in a separate building in order to reduce the chance of contamination from high-copy DNA tissue sources. For most tissue samples, an approximately 850 bp region of cyt *b* was amplified using the primers L-14115 (5′-GATATGAAAAACCATCGTTG-3′) and H-14963 (5′-GGCAAATAGGAARTATCATT-3′; Sullivan et al., 2000). To increase the success of amplifications from museum skins, three additional internal primers (two *Tamias*-specific and one universal) were used to amplify smaller regions. These primers included H-14899 (5′-TCTGGGTCTCCAAGGAGGT-3′; Good and Sullivan, 2001), L-14623 (5′-TCTACTAGTGTTGTTCCGATGTATGG-3′; this study), and L-14553 (5′-CTACCATGAGGACAAATATC-3′; Sullivan et al., 1997). PCR profiles for both tissue and skin samples were 35–40 cycles: 94 °C (30 s), 48–50 °C (30 s), 72 °C (1 min). Negative controls were run with all amplifications. Double-stranded PCR products were purified using either a 20% PEG/2.5 M NaCl solution or Qiagen QIAquick Spin Columns and cycle sequenced using the primers described above. Cycle sequenced products were purified using 5% Sephadex G-50 and sequence was collected on an ABI 377 automated sequencer (Applied Biosystems). Sequences were edited, compiled, and aligned using Sequencher, version 3.0 (Gene Codes, 1995). No insertions or deletions were observed during alignment. New sequences ($n = 151$) generated for this study were assigned the GenBank Accession Nos. AY120940–AY121090.

2.3. Phylogenetic analyses

The complete data set ($n = 165$) included the first 720 bp of cyt *b* except for two sequences from Piaggio and Spicer (2001), GenBank Accession Nos. AF147633 and AF147629, which were missing the first 8 and 19 bp, respectively. Phylogenies were estimated under frameworks of parsimony and maximum likelihood (ML) using PAUP*v4.0b4a (Swofford, 2001). An initial analysis of all sequences was conducted using equal-weight parsimony (heuristic search, 10 random addition replicates, tree bisection–reconnection (TBR) branch swapping). Nodal support was estimated with 500 parsimony bootstrap replicates with the MAXTREES option set to 10 (Felsenstein, 1985).

To reduce the computational demands of ML, the data set was pruned to 58 unique haplotypes. An equal-weight parsimony search (heuristic search, 10 random addition replicates, TBR branch swapping) recovered 149 most parsimonious trees; one of which was randomly selected as the starting topology for the subsequent evaluation of 16 nested models of sequence substitution (e.g., Sullivan et al., 1997). Four general models of nucleotide substitution were evaluated: JC (Jukes and Cantor, 1969), K2P (Kimura, 1980), HKY85 (Hasegawa et al., 1985), and GTR (Lanavé et al., 1984). In addition, different rate- heterogeneity parameters were incorporated into the models including rates among all sites assumed to vary following a discrete Γ distribution (Yang, 1994), some sites assumed to be invariable (Hasegawa et al., 1985), and a mixed distribution model of invariable sites plus Γ-distributed rates (Gu et al., 1995). The best-fit model of substitution for the data set was then determined by the likelihood-ratio test under a χ^2-approximation of the null distribution (Yang et al., 1995).

Comparisons of hierarchical-nested models of substitution allow an objective choice of the best-fit model from among those evaluated. However, this approach does not provide insight regarding the absolute goodness-of-fit between the chosen model and the data set (Goldman, 1993). To address how well the chosen model (GTR+Γ, see Section 3) actually described the cyt *b* data, we performed a parametric-bootstrap analysis (Goldman, 1993; Sullivan et al., 2000). In this approach, the difference between the likelihood of the best ML tree and the unconstrained (multinomial) likelihood score provides a test statistic (δ). This can then be compared to the distribution generated by simulation (400 replicate data sets) under the null hypothesis of a perfect fit between the data and the chosen model.

Once the model of substitution was determined to be appropriate, a successive-approximations approach to ML estimation was conducted (e.g., Sullivan et al., 1997). Nodal support for the ML tree was estimated by bootstrap analyses. One hundred ML (MAXTREES = 1) and 500 parsimony (MAXTREES = 100) replicates were conducted for bootstrap estimation. Setting the ML bootstrap estimation to a maximum of one tree per replicate to ease computational constraints has been shown not to bias bootstrap estimates (Debry and Olmstead, 2000). We also tested the molecular clock hypothesis using a likelihood-ratio test (Felsenstein, 1988).

2.4. Nested clade analyses

Nested clade analysis (NCA) was conducted in order to provide a rigorous, statistical examination of popu-

lation-level processes and haplotype association with geography (Templeton, 1998; Templeton et al., 1995). Non-random events such as restricted gene flow, range expansion, and population fragmentation can be difficult to infer based on only a visual inspection of parsimony and ML topologies. NCA incorporates a statistical methodology that allows inference of these events and a determination of the adequacy of sampling based on overall sample size, haplotype diversity, and geography (Templeton, 1998). TCS (v1.6; Clement et al., 2000) was used to construct minimum-spanning haplotype networks, based on absolute pairwise substitution differences, using all *T. amoenus* sequences ($n = 147$, excluding clades M and N; Section 3). Most parsimonious haplotype connections (probability $\geqslant 0.95$) were calculated in TCS using the method described in Templeton et al. (1992). Each network was then nested, hierarchically, into clades following guidelines in Templeton et al. (1987) and Templeton and Sing (1993). Connection ambiguities between haplotypes, resulting from homoplasy, were left unresolved and those clades were included in the next nesting level.

Nesting hierarchy, haplotype frequency, and geographic information (latitude and longitude) associated with haplotypes (Appendix A) provided the basis for the next set of analyses. For some sampling sites, precise coordinates were not available from the original locality information. In the absence of this information, coordinates were determined using three geographically oriented web sites (mapping.usgs.gov/www/gnis, www.gdbc.gov.bc.ca/bcnames, and www.juggling.org/bin/do/map-find). Although there may be some error associated with the posterior determination of latitude and longitude, the impact should be minimal given the geographic scale of our analyses. NCA was conducted using GeoDis (v2.0; Posada et al., 2000) and two tests were performed. The first, a simple contingency test, determined the significance of the association between haplotypes and geography without incorporating geographic distances. Under the null hypothesis of no geographic association of haplotypes, the observed χ^2 test statistic was compared to the null distribution generated by 10,000 permutations of random assignment of haplotypes to sample sites. The second set of calculations incorporated geographic distances between sample sites by the estimation of clade distance (D_c) and nested clade distance (D_n) values. D_c is the geographical dispersion of a clade based on the weighted average distance of haplotypes from the geographic center of the clade. D_n is a measure of the average distance of individuals comprising one clade from the geographic center of the next immediately inclusive higher clade. D_c and D_n values were also calculated for some interior versus tip (I–T) comparisons under the assumption, based on coalescent theory, that tip clades represent younger haplotypes and interior clades are composed of older haplotypes (Castelloe and Templeton, 1994). These statistics were then compared to the differing expectations of various models of population history (Templeton, 1998). A modified key based on Templeton (1998) was used to guide inference of these models (e.g., range expansion, past fragmentation) from those clades determined to have statistically significant geographic structure. The modified key is available at zoology.byu.edu/crandall_lab/geodis.htm.

3. Results

3.1. DNA sequence variation

Sequences included the first 720 nucleotides (240 codons) of cyt *b* (*Mus* positions 14,139–14,858, GenBank Accession No. J01420, Bibb et al., 1981). Nucleotide composition followed patterns observed in most mammals (Irwin et al., 1991), including other sciurids (Steppan et al., 1999). This consisted of an overall deficit of guanines (12.8%), relative to other nucleotides, most pronounced at 3rd position sites (1.6%). Base frequencies did not vary among sequences. There were 211 nucleotide sites observed to vary, 157 of which were parsimony informative. Variation was most pronounced at 1st (14%) and 3rd (85%) positions, which contained 99% of the overall variation. Maximum uncorrected sequence divergence ranged to 17.36% between *T. sibiricus* /ingroup taxa and 10.56% for ingroup comparisons (*T. dorsalis*/*T. siskiyou*). Maximum uncorrected sequence divergence within *T. amoenus* (excluding clades M and N, see below) was ~7.4% between clades J and L. Comparisons of clades M and N, which represent two subspecies of *T. amoenus* (*T. a. canicaudus* and *T. a. cratericus*), with remaining *T. amoenus* sequences ranged to 8.89 and 8.61%, respectively. Variation within *T. amoenus* was greater than many interspecific comparisons in the data set (e.g., *T. minimus*/*T. ruficaudus*, 5.42%; *T. minimus*/*T. speciosus*, 5.69%). Among 147 sequences of *T. amoenus* (excluding clades M and N) 63 unique haplotypes were identified. Nuclear copies of mtDNA genes (pseudogenes) have been documented in some species of mammals (Smith et al., 1992); however, characteristics of pseudogenes, such as a relaxation of compositional biases, truncated sequences, stop codons, or frameshift mutations were not observed in our data.

3.2. Phylogenetic analyses

The equal-weight parsimony search with the complete data set ($n = 165$) recovered 103 most parsimonious trees of 542 steps (consistency index = 0.456, retention index = 0.910, rescaled consistency index = 0.415). Fourteen clades containing *T. amoenus* were designated A–N based on $\geqslant$85% bootstrap support (Fig. 2). Two clades, M and N, are not nested with

remaining samples of *T. amoenus* (clades A–L) but group with other species of *Tamias*. Clade M, representing *T. a. cratericus*, was sister to *T. speciosus* (59%) and clade N, representing *T. a. canicaudus*, grouped with *T. ruficaudus* (82%). The 12 remaining clades of *T. amoenus* (A–L) are depicted as monophyletic in Fig. 2 and sister to the 3 species of the *T. townsendii* group (Fig. 2), however this relationship is characterized by <50% bootstrap support. This is highlighted by the observation that the major difference among the 103 most parsimonious trees is the position of clade L as either basal (56 trees) to clades A–K (Fig. 2) or as sister to the *T. townsendii* group. Clades A–K comprise a moderately supported (77%) group characterized by weak support (<50%) for many interclade relationships (Fig. 2). Several interspecific clades that correspond to the mtDNA species groups identified by Piaggio and Spicer (2001) are also apparent in the parsimony tree (Fig. 2). These include the *T. townsendii* group (*T. townsendii*, *T. senex*, and *T. siskiyou*), *T. merriami* (*T. merriami* group), and the *T. quadrivittatus* group (*T. dorsalis* and *T. umbrinus*). Weak bootstrap support (<50%) characterizes relationships between the remaining species (*T. minimus*, *T. ruficaudus*, and *T. speciosus*) and *T. amoenus* clades M and N.

Among the models of substitution evaluated for ML, GTR + I + Γ had the best likelihood score ($\ln L = -3380.4533$). However the GTR + Γ model, with one less free parameter, was not significantly worse ($\ln L = -3381.5543$; $\chi^2_1 = 2.2, 0.5 > P > 0.1$). The result of the parametric bootstrap test to assess goodness-of-fit between the GTR + Γ model and the data indicates that the model fits the data adequately. The test statistic for the real data ($\delta = 1197.9957; P = 0.07$) falls within the distribution of 400 simulated data sets generated under the null hypothesis of a perfect fit between the model and data (Fig. 3). After the successive-approximations approach using the GTR + Γ model (final parameter estimates: $r_{AC} = 10.09$, $r_{AG} = 144.20$, $r_{AT} = 9.65$, $r_{CG} = 5.88 \times 10^{-9}$, $r_{CT} = 200.00$, $r_{GT} = 1.00$; $\alpha = 0.12481$), one ML tree was recovered ($\ln L = -3371.7650$; Fig. 4).

The ML tree was similar to the parsimony tree (Fig. 2) with regard to the recovery of the same well-supported clades (A–N) corresponding to *T. amoenus* haplotypes. Monophyly of *T. amoenus* clades A–L was moderately supported by ML bootstrap (61%). As in the parsimony tree, clades M and N, representing the subspecies *T. a. canicuadus* and *T. a. cratericus*, nested outside of clades A–L and with other species of *Tamias* (Fig. 4). Relationships among clades A–I differed somewhat from the parsimony tree and this is reflected by the low bootstrap values observed for many of the internal nodes in both trees (Figs. 2 and 4). Clades representing several species groups also were recovered in the ML tree, however a monophyletic *T. minimus* group (*T. minimus* and *T. ruficaudus*) was not recovered. A molecular clock for the reduced data set was rejected ($\chi^2_{56} = 122.6734$; $P < 0.001$).

The geographic distributions of clades A–L do not generally correspond to existing subspecific boundaries (Fig. 1), rather they correspond to distinct mountain ranges as depicted on the area cladogram derived from the ML topology and associated map of clade distributions (Fig. 5). This includes clade A, which is restricted to the Cascade Range in Oregon/Washington and the Olympic Mountains. Clade B includes haplotypes from the Cascade Range in Washington trending north into British Columbia into the Coast Mountains and Fraser Plateau. One sample site (46) in the Washington Cascade Range has both A and B haplotypes. The tri-state region of southeastern Washington, northeastern Oregon and west central Idaho represents an area where three non-sister clades, C, D, and K, are in close proximity, but are restricted to the Craig/Wallowa Mountains, northern Blue Mountains, and Seven Devils Mountains, respectively. Another region of high clade diversity includes southcentral Oregon and northern California where a single individual of clade E (SOU2369) and clades G, H, and I are centered on the Sierra Nevada Mountains, southern Cascade Range, and southern Cascade Range/Oregon Highlands, respectively. Sister clades, E and F, represent populations from the Oregon Highlands (E), southern Idaho (F), northern Utah (F—Raft River Mountains), and Beartooth Mountains (F) in northwestern Wyoming. Clade J (sister to clade K) includes populations from the Beartooth, Bitterroot, Clearwater, Garnet, Highland, Sawtooth and Teton mountains of Idaho, Montana, and Wyoming. Clade L, the most basal clade within the A–L assemblage, includes populations from the Columbia Mountains and Okanogan Highlands of northwestern Montana, southeastern British Columbia, and northeastern Washington.

3.3. Nested clade analyses

Based on the 0.95-connection probability ($\leqslant$11 substitutions) calculated by TCS (Clement et al., 2000), haplotypes of *T. amoenus* (excluding clades M and N) were subdivided into six networks (Fig. 6). These included networks ABEF ($n = 57$), network C ($n = 15$), network D ($n = 4$), network GHI ($n = 14$), network JK ($n = 32$), and network L ($n = 25$). Due to ambiguities associated with resolution of relationships among the clades (Figs. 2 and 4), we did not connect networks beyond the limits of the 0.95-connection probability. With the exception of the 5-step network, ABEF, networks generally correspond to relationships among well-supported clades revealed by parsimony and ML analyses (Figs. 2 and 4). Incongruence between NCA and tree-estimation methods involves areas of low bootstrap support (Fig. 2) and NCA connections close

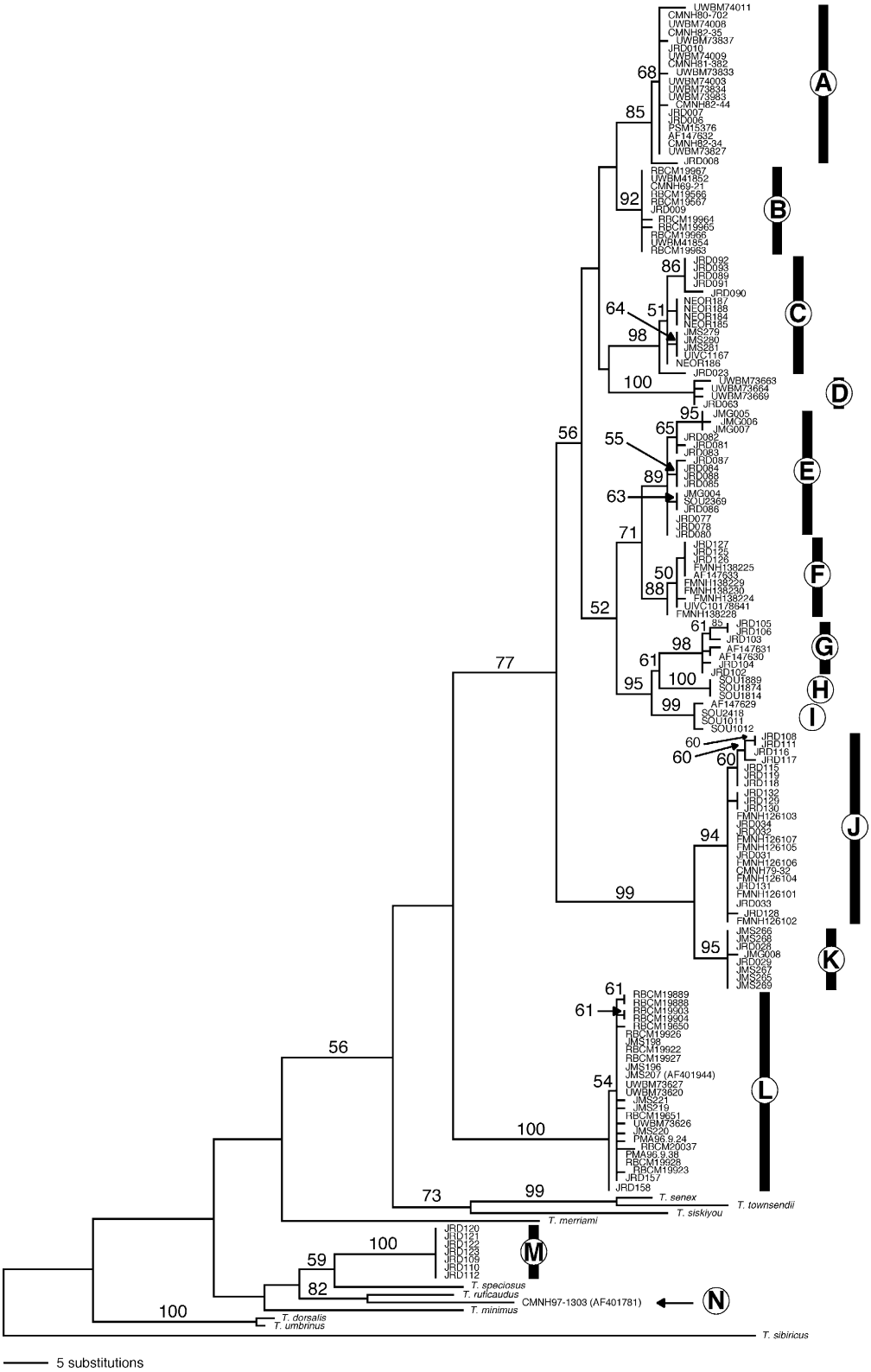

Fig. 2. One of 103 most parsimonious trees (542 steps, consistency index = 0.456, retention index = 0.910, rescaled consistency index = 0.415) found with an equal-weight search including all sequences ($n = 165$). The tree was rooted with *T. sibiricus*. Branch lengths were inferred under ACCTRAN and bootstrap values >50% (500 replicates) are shown above the branches. Clades discussed in the text and corresponding to samples of *T. amoenus* are labeled A–N. The major difference among the 103 trees was the position of clade L as basal to clades A–K, as depicted, or as sister to the *T. townsendii* group clade.

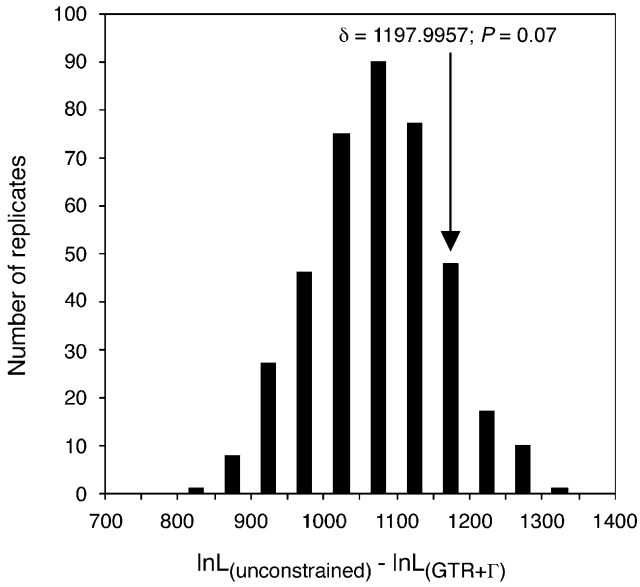

Fig. 3. The parametric bootstrap test to assess the absolute goodness-of-fit between the objectively determined GTR + Γ model of substitution and the cyt *b* data ($n = 58$). Four hundred replicate data sets were simulated under the GTR + Γ model and the null distribution was determined based on the difference between the unconstrained (multinomial) likelihoods and the likelihood of the ML tree under the model. For the GTR + Γ model, the test statistic of 1197.9957 falls within the simulated null distribution indicating good fit between the model and cyt *b* data ($P = 0.07$).

to the limits of the 0.95-connection probability (Fig. 6). Clades D, M, and N were not included in further analysis due to small sample sizes representing limited geographic sampling. The nesting contingency test indicated that of 24 nested clades analyzed, 10 were significantly associated with geography (Table 1). The modified inference key of Templeton (1998) was used to identify population-level processes associated with the 10 clades that exhibited significant geographic association and the results are summarized in Table 2.

Network ABEF (equivalent to nested clade 5.1) consisted of 21 sampled haplotypes (57 individuals) comprising a 5-step network (Fig. 6). Five of the 12 nested clades, 2.11, 3.4, 4.1, 4.2, and 5.1, were significantly associated with geography. Nested clades 2.11 and 3.4, representing central Oregon Highlands haplotypes (E), exhibited the signatures of restricted gene flow with isolation by distance (Table 2). Objective assignments of interior or tip status within higher-level clades 4.1, 4.2, and 5.1 was unclear due to deeper connection ambiguities as described above, and strict adherence to the inference key led to inconclusive results. However, given the arid, lowland areas (Fig. 5) between the distribution of many of these clades coupled with the divergence among them, we postulate that past vicariance has most likely produced the pattern apparent in these phylogeographic relationships. In the case of clades A and B (nested clade 4.2) there is probably substantial overlap in their haplotype distributions as evidenced by our sampling of site 46. This might represent secondary contact between clades A and B; expanded sampling in the Cascade Range would be required to address this issue.

Clade 2.4 of network C (15 individuals, 6 haplotypes) included the geographically restricted interior clades 1.7, 1.8, and 1.9. This network, which included haplotypes from the Craig and Wallowa Mountains, is hampered by a lack of geographic sampling that does not allow us to distinguish between range expansion and isolation by distance (Table 2). Clade 3.2 of network GHI (14 individuals, 10 haplotypes) also included the geographically restricted interior clade, 2.6, and exhibited the signature of contiguous range expansion. Network JK (32 individuals, 9 haplotypes) was composed of three nested clades that exhibited significant geographic association (1.4, 2.3, and 3.1). Due to inadequate sampling, NCA was unable to differentiate between events of past fragmentation or isolation by distance within network J composed of clades 1.4 and 2.3 (Table 2). At the next inclusive clade, 3.1 (network JK), past fragmentation between haplotypes J and K was inferred, corresponding to the isolation of the Seven Devils Mountains from the central Idaho ranges (Fig. 5).

4. Discussion

Many morphological characters, such as pelage or cranial features, may be prone to convergence among non-sister taxa in response to rapid, local adaptation. This has been observed as a recurring phenomenon in *Tamias* (Levenson et al., 1985). Thus, independent molecular markers less prone to this phenomenon are often required to resolve underlying phylogenetic relationships. In this regard, mitochondrial genes such as cyt *b* have been proven effective towards achieving this goal at intraspecific levels (e.g., Demboski and Cook, 2001; Harris et al., 2000). In this study, the combination of tree-building and network methods suggests new insights regarding the evolutionary history of *T. amoenus*. These include: (1) differentiation within *T. amoenus* not suggested by current taxonomy, (2) two subspecies, *T. a. canicaudus* and *T. a. cratericus*, that nest well outside of other *T. amoenus* haplotypes in topologies, (3) lack of concordance of well-differentiated clades with established subspecific distributions, but geographic concordance with discrete mountain ranges, and (4) signatures of different population-level processes structuring genetic variation within particular clades.

4.1. Systematics

There has been much effort directed at resolving phylogenetic relationships within *Tamias*. Different morphological (Levenson et al., 1985), biochemical

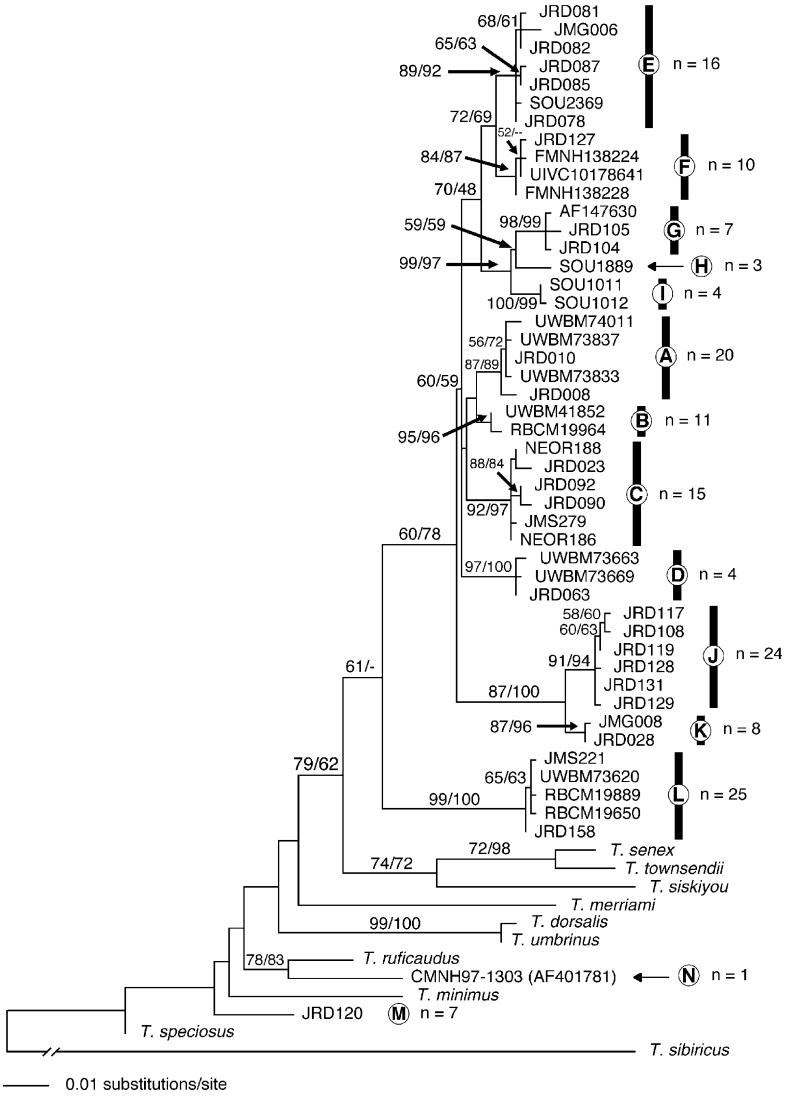

Fig. 4. The maximum likelihood topology ($\ln L = -3371.765$) estimated under the GTR + Γ model of substitution with only unique *T. amoenus* haplotypes and 10 additional species of *Tamias* ($n = 58$) included. The tree was rooted with *T. sibiricus*. ML (100 replicates) and parsimony (500 replicates) bootstrap values >50%, respectively, are shown on the branches. Clades discussed in the text and corresponding to samples of *T. amoenus* are labeled A–N. Numbers following clades indicate the total number of individuals belonging to each clade.

(Ellis and Maxson, 1979; Levenson et al., 1985), chromosomal (Nadler et al., 1977), host/ectoparasite (Jameson, 1999), and molecular (Piaggio and Spicer, 2000, 2001) studies have recognized three distinct groups within *Tamias*, *T. sibiricus*, *T. striatus*, and the 23 western North America species. Debate continues regarding assignment of either generic or subgeneric status to these groups, but regardless of taxonomic designations, 3–5 species groups within the western North America chipmunks have been recognized (Howell, 1929; Levenson et al., 1985; Piaggio and Spicer, 2000; White, 1953). Unfortunately, lack of resolution among internal nodes within the monophyletic western North America clade has prevented firm conclusions about species-group relationships (Piaggio and Spicer, 2000). It is apparent from allozyme (Levenson et al., 1985) and mtDNA sequence data (Piaggio and Spicer, 2000) that some widespread species (e.g., *T. minimus*) may be para- or polyphyletic composites of species. Our analyses confirm many of these previous observations and highlight the difficulty of inferring species-group relationships within *Tamias*.

We included 10 additional species of *Tamias* in our analysis of *T. amoenus* for several reasons. First, we wanted to determine the appropriate sister taxa for *T. amoenus*. Second, inclusion of *T. amoenus* populations representing sequence divergence from 4 to 9% (clades JK, L, M, and N) suggested the possibility of cryptic lineages. Third, we wanted to eliminate potential taxonomic misidentifications with other species found in sympatry with *T. amoenus*. With the exception of the *T. minimus* group, taxa assigned to distinct species groups

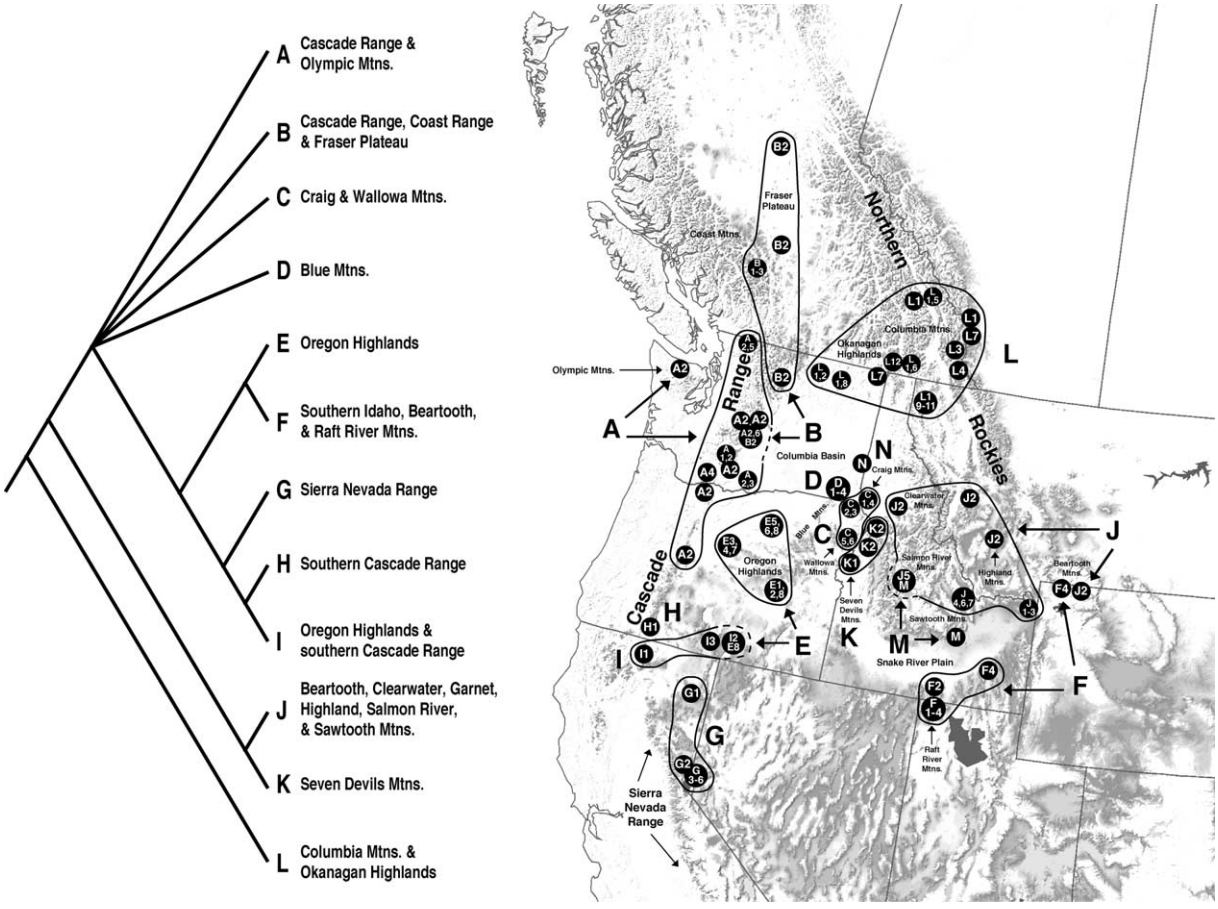

Fig. 5. Area cladogram and map of western North America depicting the distribution of major clades of *T. amoenus* recovered with parsimony and ML (Figs. 2 and 4). Topology and nodal support ($\geqslant$50% ML bootstrap) follow Fig. 4. Major clade (A–L) distributions, haplotype associations, and associated mountain ranges are depicted on the cladogram and on the map. Refer to Fig. 1 for *T. amoenus* distribution, subspecific boundaries, and sampling site localities.

by Piaggio and Spicer (2000) were differentiated in both our parsimony and ML topologies, however relationships among species groups were weakly supported confirming their earlier conclusions. This included recovery of the *T. townsendii* group (*T. townsendii*, *T. senex*, and *T. siskiyou*), the *T. merriami* group (*T. merriami*), and the *T. quadrivittatus* group (*T. dorsalis* and *T. umbrinus*). A monophyletic *T. minimus* group was recovered in the parsimony tree with weak bootstrap support (Fig. 2) and included *T. minimus* from Wyoming, *T. ruficaudus*, *T. speciosus* and two *T. amoenus* clades (M and N; discussed below). This clade was not recovered in the ML analysis (Fig. 4) and suggests that phylogenetic relationships among taxa assigned to this species group are complex, requiring extensive sampling of *T. minimus* and sister taxa. Our results, with the exception of clades M and N (see below) and possibly clade L, confirm the conclusions of Piaggio and Spicer (2000, 2001) that *T. amoenus* haplotypes (clades A–K) represent a monotypic species group within western North America species of *Tamias*. The ML topology also indicates a sister relationship supported by moderate bootstrap values with the *T. townsendii* group composed of *T. senex*, *T. siskiyou*, and *T. townsendii* (Fig. 4). These conclusions are tentative given our limited sampling of 11 species in *Tamias* and our primary focus on examining intraspecific relationships in *T. amoenus*.

Within *T. amoenus*, parsimony and ML topologies depict several examples of high sequence divergence. First, we discuss observations for the larger inclusive clade A–L, which represents a weakly supported monophyletic group in the ML topology (Fig. 4). The basal clades, JK and L, exhibit high levels of uncorrected cyt *b* divergence when compared to each other (~6–7%) and to clades A–I (4.5–6.5%). Clades JK and L consist of populations that are distributed in the eastern part of the distribution of *T. amoenus* (Fig. 5). The observed levels of divergence are comparable to or greater than many interspecific comparisons (e.g., *T. minimus*/*T. ruficaudus*, 5.4%; *T. minimus*/*T. speciosus*, 5.7%) in our data set. Although genetic distances have been suggested as a general yardstick for taxonomic designations (e.g., Avise and Johns, 1999), in the ab-

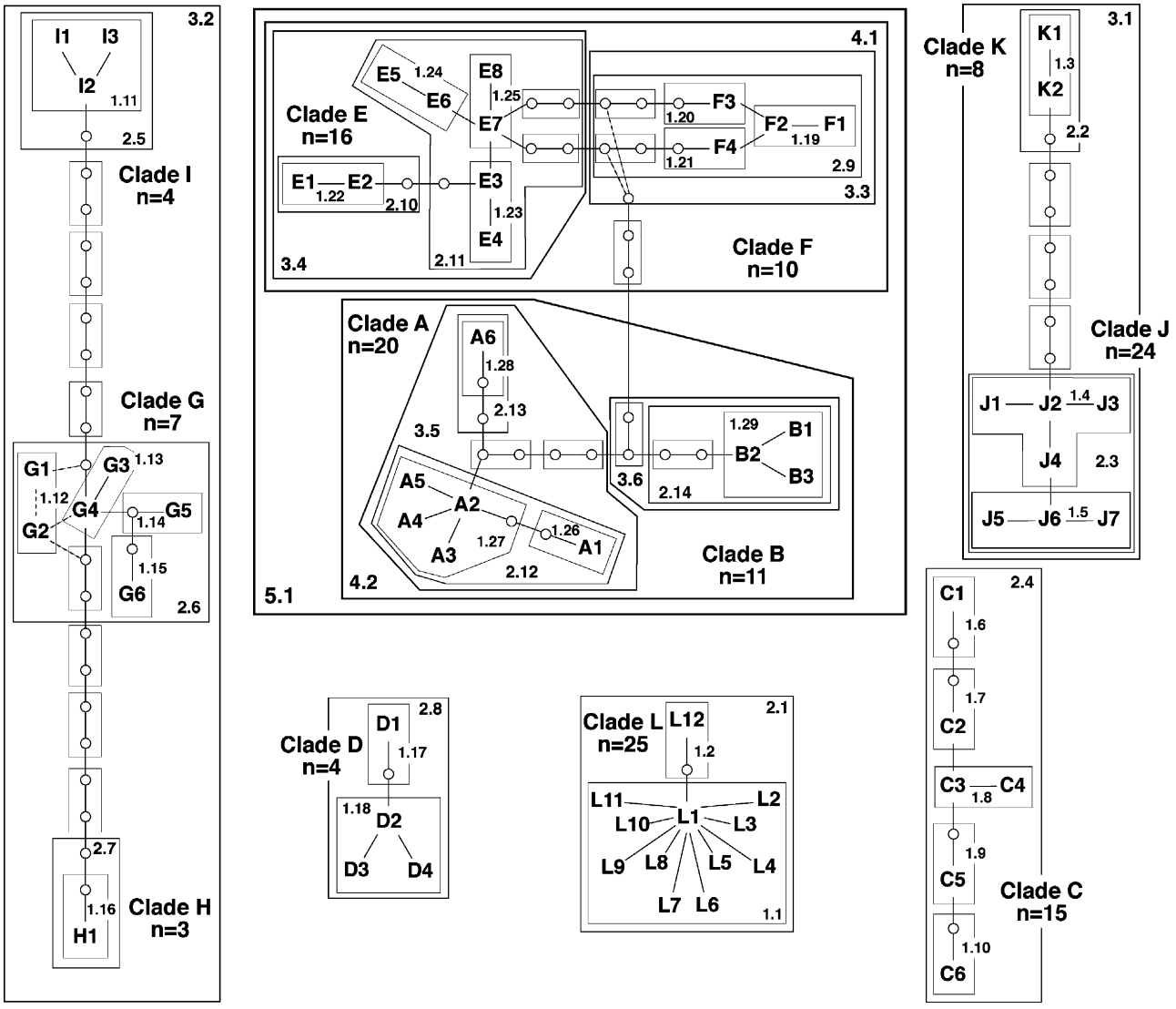

Fig. 6. The nested haplotype networks for *T. amoenus* clades A–L. Haplotype connections ($\leqslant$11 substitutions) are based on a $\geqslant$0.95 probability of being parsimonious. Branches connecting haplotypes represent single substitutions. Circles represent unsampled haplotypes. Closed loops (dashed lines) represent ambiguous connections resulting from homoplasy. Hierarchical nesting levels are denoted by boxes and numbered clades. Haplotypes (e.g., L1) and associated specimens are summarized in the Appendix A and geographically depicted on Fig. 5.

sence of evidence from additional independent characters, it would be premature to suggest elevation of one or more of these clades to specific level. However, given the extensive range of cyt *b* divergence within *T. amoenus*, it is likely that analyses of other genes (e.g., nuclear) will support our cyt *b* observations.

Although our sampling was not necessarily directed towards the goal of re-examining subspecific taxonomy within *T. amoenus*, we are provided with some initial insight regarding this question. We were able to sample 10 of the 14 recognized subspecies (Fig. 1). Two subspecies were not sampled, *T. a. celeris* and *T. a. septentrionalis*, however it is not clear if specimens representing *T. a. ochraceus* and *T. a. vallicola* were actually sampled. These sampling sites (26 and 34; Fig. 1) are located near subspecific boundaries which in many cases were originally determined in somewhat arbitrary fashion. Regardless of the number of the subspecies we sampled, it is apparent that overall geographic partitioning of cyt *b* haplotypes does not follow groups suggested by subspecific taxonomy, rather it appears tied to mountain topography. For example, the isolated Olympic Mountains subspecies (sample site 42), *T. a. caurinus*, is indistinguishable from Cascade Range haplotypes (clade A). The distribution of the widespread subspecies, *T. a. luteiventris*, includes haplotypes belonging to 4 non-monophyletic clades (F, J, K, and L; Figs. 1 and 5). These observations are not surprising given that the majority of *T. amoenus* subspecies were described in the late-19th and early-20th centuries (Sutton, 1992) based on characters, such as pelage coloration and body size, which are known to be subject to

Table 1
Contingency tests of Geographic Association

Network	Nested clades	χ^2-Statistic (probability)
ABEF	1.19	0.444 (1.000)
	1.25	6.000 (0.101)
	1.27	30.083 (0.538)
	1.29	2.993 (1.000)
	2.9	7.400 (0.296)
	2.11	**11.917 (0.020)**
	2.12	5.965 (0.800)
	3.4	**11.077 (0.008)**
	3.5	9.975 (0.382)
	4.1	**26.000 (0.000)**
	4.2	**27.506 (0.001)**
	5.1	**56.000 (0.000)**
C	1.8	5.000 (0.200)
	2.4	**25.200 (<0.000)**
D	Not analyzed	Not determined
GHI	1.11	8.000 (0.168)
	2.6	14.000 (0.478)
	3.2	**24.000 (0.009)**
JK	1.3	8.000 (0.121)
	1.4	**34.770 (0.004)**
	1.5	4.000 (0.334)
	2.3	**15.360 (0.012)**
	3.1	**32.000 (0.000)**
L	1.1	123.667 (0.0074)
	2.1	25.000 (0.078)
M	Not analyzed	Not determined
N	Not analyzed	Not determined

Note. Significant values (0.05 level) under the null hypothesis of no association of haplotypes with geography are shown in bold.

rapid adaptation in *Tamias* (Levenson et al., 1985; Piaggio and Spicer, 2001). This lack of geographic congruence also extends to higher-level phylogenetic incongruence with two purported subspecies.

Two clades, M and N, are not nested within remaining clades of *T. amoenus* (Figs. 2 and 4). These clades include samples that have been assigned to the subspecies, *T. a. canicaudus* (N) and *T. a. cratericus* (M). The distribution of *T. a. canicaudus* is throughout the semi-xeric Palouse region (central Washington and northcentral Idaho) with records in western Montana (Hall, 1981). We sampled one individual (CMNH97-1303) from eastern Washington (sample site 55) classified as *T. a. caniaudus* based on Hall (1981). This individual possesses *T. amoenus*-like pelage coloration and bacular (os penis) characteristics (Merriam, 1903); however, a sister relationship to the red-tailed chipmunk (*T. ruficaudus*) is indicated in both parsimony and ML trees (Figs. 2 and 4). Analysis of 14 individuals from sample site 55 by Good and Sullivan (2001) indicates that these samples comprise a well-supported clade (Palouse clade) nested within the red-tailed chipmunk, *T. ruficaudus*, and are sister to the western subspecies, *T. r. simulans*. Given the preliminary results of expanded sampling of *T. a. canicuadus* ($n = 46$), we suggest that this represents asymmetric introgression and subsequent fixation of mtDNA as a result of a historic hybridization event (Good et al., in press).

The second example (clade N) involves the restricted subspecies, *T. a. cratericus*, from on and around Craters of the Moon National Monument in southern Idaho (sample site 16). This subspecies was originally described based on external measurements and pelage coloration by Blossom (1937). Our examination of four topotypes sampled from the Monument campground, shows clade N nested well outside other *T. amoenus* sequences (Figs. 2 and 4). In addition, three individuals from sample location 19 (Idaho, Custer Co.) possess cyt *b* haplotypes identical to those from location 16. This high-elevation site also includes two individuals (haplotype J5) sampled from the same trap line. White (1953) and Sutton (1982) both commented on the bacular morphology of *T. a. cratericus* (and on individuals from other locations in southern Idaho) and suggested that was not similar to other *T. amoenus*. This supports our conclusion that minimally, *T. a. cratericus* is not a subspecies of *T. amoenus*. Indeed, these haplotypes do not appear to be closely related to any species included in our study (Fig. 4). Additional sampling in southern Idaho south of the Salmon River may clarify these findings.

4.2. Phylogeography

It is well established that northwest North America has undergone remarkable topographic change because of past geologic and climatic events. These events, which include orogeny, climatic fluctuations, and repeated expansion/recession of continental ice sheets and habitats, have had dramatic effects upon the genetic structuring of flora and fauna in the region. This is becoming more apparent from other molecular studies (e.g., Brunsfeld et al., 2001; Cook et al., 2001; Soltis et al., 1997). Major events in the region include the uplift of the Rocky Mountains during the Eocene (45–36 Mya) followed by a sharp decrease in average temperatures during the Oligocene (~33 Mya) into the present (Wolfe, 1978). The orogeny of the Cascade and Sierra ranges during the Pliocene (5–2 Mya) created the rain shadow presently in place across the Columbia Plateau and northern Great Basin (Graham, 1999) separating these ranges from the northern Rocky Mountains. During the Pleistocene, repeated movement of continental ice sheets in response to Milankovitch cycles rendered much of the northwestern North America unavailable to flora and fauna (Delcourt and Delcourt, 1993). Although not as extreme as in previous epochs, climatic oscillations during the Holocene also impacted taxa (Hadley, 1996). Determining calibration points for estimating dates of divergence within *T. amoenus* is difficult. Fossils of *T. amoenus* have not been identified (Sutton, 1992) and unambiguous fossils assigned to extant species of the genus *Tamias* are also lacking. In

Table 2
Results of the nested clade analysis

Network	Nested clades	Inclusive clades	D_c	D_n	Inference chain; population inference
ABEF	2.11 (E)	1.23 (Interior)	0	74	1–2–3–4–No; Restricted gene flow with isolation by distance
		1.24 (Tip)	**0**^{S}	114	
		1.25 (Interior)	113	123	
		I–T	**75**^{L}	−7	
	3.4 (E)	2.10 (Tip)	0	**61**^{S}	1–2–3–4–No; Restricted gene flow with isolation by distance
		2.11 (Interior)	**113**^{L}	**115**^{L}	
		I–T	**113**^{L}	**54**^{L}	
	4.1 (EF)	3.3 (NA)	**146**^{S}	332	1–2–Inconclusive; Past fragmentation?
		3.4 (NA)	**105**^{S}	317	
		I–T	NA	NA	
	4.2 (AB)	3.5 (NA)	**133**^{S}	**168**^{S}	1–2–Inconclusive; Past fragmentation with secondary contact?
		3.6 (NA)	202	**336**^{L}	
		I–T	NA	NA	
	5.1 (ABEF)	4.1 (NA)	324	**486**^{L}	1–2–Inconclusive; Past fragmentation?
		4.2 (NA)	**215**^{S}	**288**^{S}	
		I–T	NA	NA	
C	2.4	1.6 (Tip)	0	51	1–2–11–12–13–14–No; Sampling inadequate to distinguish between contiguous range expansion or isolation by distance
		1.7 (Interior)	**0**^{S}	**26**^{S}	
		1.8 (Interior)	**13**^{S}	46	
		1.9 (Interior)	**0**^{S}	**70**^{L}	
		1.10 (Tip)	0	70	
		I–T	**5**^{S}	−13	
GHI	3.2	2.5 (Tip)	87	157	1–2–11–12–No; Contiguous range expansion
		2.7 (Tip)	0	183	
		2.6 (Interior)	**91**^{S}	135	
		I–T	22	−28	
JK	1.4 (J)	J1 (Tip)	0	150	1–2–3–4–9–10–No; Geographic sampling inadequate to distinguish between geographic fragmentation or isolation by distance
		J2 (Interior)	155	171	
		J3 (Tip)	**0**^{S}	150	
		J4 (Interior)	**0**^{S}	122	
		I–T	126	12	
	2.3 (J)	1.4 (Interior)	162	167	1–2–3–4–9–10–No; Geographic sampling inadequate to distinguish between geographic fragmentation or isolation by distance
		1.5 (Tip)	**56**^{S}	150	
		I–T	106	17	
	3.1 (JK)	2.2 (Tip)	**30**^{S}	189	1–2–3–4–9–No; Past geographic fragmentation
		2.3 (Interior)	**164**^{S}	175	
		I–T	**134**^{L}	−14	

Note. Analyses were limited only to the 10 nested clades exhibiting a significant association with geography (see Table 1). Clades within each nested clade and their associated interior or tip designation are listed. Values for clade distance (D_c) and nested clade distance (D_n) in kilometers are included. Interior versus tip contrasts (I–T) are also reported where applicable. Significantly large (^{L}) or small (^{S}) values of D_c or D_n are shown in bold. The inference chain and population inferences follow from the modified inference key (see text) of Templeton (1998). For clades where interior and tip designations were not determined (4.1, 4.2, and 5.1), determinations of population process were suggested without using the inference key.

addition, our rejection of a molecular clock for our data precludes assignment of dates regardless of the availability of independent calibration points for *Tamias*. However, it is evident that the levels of uncorrected divergence (~4.5–7.4%) observed within *T. amoenus* probably represent diversification events that occurred before the Late Pleistocene.

The complex phylogeographic patterns within *T. amoenus* are particularly striking given the tight association of genetic structure with geography (Fig. 5). Clades A–L are restricted to distinct mountain ranges or biogeoclimatic zones in northwestern North America. This is not surprising given the dependence of *T. amoenus* on forested habitat and is actually a more plausible explanation of phylogeographic patterns than current subspecific designations based on morphology. Since many of the mountain ranges in western North America are isolated by large non-forested regions, it is evident that vicariance has played a major role in shaping the phylogeography of *T. amoenus* and continues to do so. At the broad scale, phylogeographic patterns within *T. amoenus* are characterized by a general east/west dichotomy with one notable exception, clade F. Clades L and JK represent basal haplotypes within *T. amoenus* located in the eastern part of its current distribution (Fig. 5). Remaining clades, A–E and G–I, are found in western mountain ranges such as the Cascade Range, Sierra Nevada Range, and Oregon Highlands. This east/

west phylogeographic signature is similar to the common coastal/inland pattern noted for a large number of taxa in northwestern North America. Approximately 170 species, representing multiple kingdoms, exhibit a general east/west dichotomy that is characterized by distribution (e.g., Dalquest, 1948; Johnson, 1987), genetics (e.g., Demboski et al., 1999; Gill et al., 1993), or both (e,g., Nielson et al., 2001). In many of these taxa, molecular studies have revealed deep, east/west divergences that are otherwise morphologically cryptic. Differences among these taxa relate to their habitat requirements, extent of extant distributions, depth of the coastal/inland divergence (Arbogast and Kenagy, 2001; Demboski et al., 1999), possession of sister lineages in the southern Rocky Mountains (Demboski and Cook, 2001), and zones formed following secondary contact (Wooding and Ward, 1997). Regardless, it is likely that the initial formation of a Cascade/Sierra Nevada rain shadow in the Pliocene has promoted this large-scale east/west dichotomy across multiple taxa in northwest North America. Not surprisingly, given extensive climatic fluctuations over the last 5 million years, this suggests a process that has occurred multiple times. Clades A–L are sister to the coastal-distributed *T. townsendii* group (Fig. 4) and this may represent the initial, deep event that isolated ancestral populations in coastal and inland refugia. A subsequent event may have again separated ancestral populations in coastal and inland refugia leading to divergence between clades A–I and JK. Conversely, the weak support for monophyly of clades A–L (Fig. 2), with clade L sister to the *T. townsendii* group in many parsimony trees (not shown) may suggest that clade L and the *T. townsendii* group represent the earliest coastal/inland divergence.

In contrast with most taxa that have been examined in northwest North America, *T. amoenus* differs by possessing a high level of observed phylogeographic structure (Fig. 5; but see Conroy and Cook, 2000). This suggests that *T. amoenus* has responded to the effects of habitat fragmentation caused by past climatic change. This is supported by the results of our NCA. At higher nesting levels (ABEF and JK), which correspond to deeper time frames, past geographic fragmentation is the inferred process that explains current haplotype distributions (Table 2). At these higher-nesting levels, clades are separated by lowland areas typically characterized by non-forested, high-desert habitats (e.g., Columbia Basin; Fig. 5). These areas apparently have served as effective barriers to dispersal and have the reinforced phylogeographic structure observed within *T. amoenus*. In addition, competitive interactions with other species of *Tamias* also may have limited *T. amoenus* dispersal. At lower-nesting levels (clades C, E, F, and GHI), range expansion and isolation by distance are the two processes inferred by NCA to explain haplotype distributions (Table 2). The lower-nesting levels characterizing these haplotypes are indicative of a shallower timeframe to coalescence. However, clades C, E, F, and GHI represent populations that are presently separated by non-forested regions between mountain ranges. For example, clade C (network 2.4) includes populations from the Wallowa (Oregon) and Craig (Idaho) mountains, which are separated by the Snake River Canyon (Fig. 5). The NCA was unable to differentiate between range expansion and isolation by distance to explain the clade C haplotype pattern. It is reasonable to conclude that this inference may represent the residual signature of a former contiguous population, consistent with more extensive forestation, in the region during the last major glacial advance. This might also be the case for clades E, F, and GHI which also now include fragmented populations. Populations in these clades have not been separated long enough for haplotype sorting to occur and thus, the effects of the present habitat fragmentation are not evident in our data. Although our sampling of clades A and L (Table 1) was insufficient to present a statistically supported inference, range expansion is the most likely cause of present haplotype patterns. Much of the current distributions of clades A and L occur in areas that were covered by the Cordilleran ice sheet during the last major glaciation. This would indicate that extant populations represent recent expansions into deglaciated areas concurrent with Holocene warming. Additional support for our conclusions based on NCA awaits further sampling of clades and an independent assessment using nuclear loci such as microsatellites.

5. Conclusions

Our results stress the importance of thorough geographic sampling when attempting to reconstruct the phylogeographic history of a species. Previously unrecognized differentiation within *T. amoenus* and apparent incongruence with existing taxonomy are evident in our study. Recent mtDNA analyses of *Tamias* (Piaggio and Spicer, 2000, 2001) did not include samples representing basal clades (J, K, and L) within *T. amoenus*, thus underestimating genetic diversity within the species and *Tamias*. It is likely that more intensive sampling of other western species of *Tamias* will reveal similar complexity as evidenced by this study. Although our data do not provide a direct evaluation of the morphological characters used for the original descriptions, current subspecific taxonomy has limited use if it does not accurately reflect underlying genetic diversity. This could have important implications for future conservation efforts. Much of the forested habitat for *T. amoenus* is on public lands in the United States and Canada and these areas have been the focus of destructive activities such as timber harvest and mining.

Our work also provides an initial framework for comparative phylogeography of the region. We are examining two additional species of mammals, the montane vole (*Microtus montanus*) and the wandering shrew (*Sorex vagrans*), both of which are generally co-distributed with *T. amoenus* in western North America. Although these three species of mammals share similar distributions, *M. montanus* and *S. vagrans* are not as restricted to forested-habitats as *T. amoenus*. This adds another dimension to comparative phylogeographic studies regarding the differing temporal roles of historical processes and more contemporary ecological responses in shaping genetic structure.

Acknowledgments

We would like to thank B. Arbogast, S. Birks, J. Rozdilsky, G. Kenagy, and S. Birks (Burke Museum of Natural History and Culture), L. Heaney and B. Patterson (Field Museum of Natural History), B. McGillivray and B. Weimann (Provincial Museum of Alberta), D. Nagorsen and N. Panter (Royal British Columbia Museum), D. Paulson (Slater Museum of Natural History), A. Sonneada (Nez Perce Tribe), K. Stone (Southern Oregon University), and S. Vander Wall (University of Nevada Reno) for specimens or loans of tissues/museum skins. T. Piaggio and G. Spicer graciously provided us with unpublished sequences of *Tamias*. We extend special thanks to J. Good, S. Gregory, and T. Rinehardt for assistance in the field. J. Good also provided continuous support and discussion of chipmunk biology. This research was supported by a grant from the NSF/Idaho EPSCoR program (EPS-9720634) to J.S. Additional support was provided by equipment grant DHHS/NIH RR11833 to the Department of Biological Sciences, University of Idaho.

Appendix A

Sample sites	*n*	Specimen ID (haplotype designation)	Locality
1	1	PMA96.9.38 (L1)	Alberta, Kananaskis Country, 2 km S Baril Creek on Highway 940, 50°20′N, 114°37′W
2	1	PMA96.9.24 (L7)	Alberta, Kananaskis Country, Wilkinson Creek, 50°13′N, 114°35′W
3	1	CMNH69-21 (B2)	British Columbia, 25 mi N Clinton, 51°24′N, 121°12′W
4	2	RBCM19903 (L3), RBCM19904 (L3)	British Columbia, 3 mi W Racehorse Pass, 49°46′N, 114°40′W
5	2	RBCM19888 (L4), RBCM19889 (L4)	British Columbia, Andy Good Creek, below Mt. Ptolemy, 49°31′N, 114°38′W
6	5	RBCM19963 (B2), RBCM19964 (B1), RBCM19965 (B3), RBCM19966 (B2), RBCM19967 (B2)	British Columbia, Cayoosh Creek, 50°30′N, 122°18′W
7	1	RBCM20037 (L12)	British Columbia, Creston Valley, W side, Topaz Creek Forestry Road, 49°10′N, 116°38′W
8	3	RBCM19926 (L1), RBCM19927 (L1), RBCM19928 (L1)	British Columbia, Delphine Mine Trail, 50°26′N, 116°22′W
9	2	RBCM19566 (B2), RBCM19567 (B2)	British Columbia, near Strathnaver, 53°17′N, 122°29′W
10	2	RBCM19922 (L1), RBCM19923 (L5)	British Columbia, Paradise Mine Road, 4.65 km from beginning of ascent, 50°28′N, 116°16′W
11	2	RBCM19650 (L6), RBCM19651 (L1)	British Columbia, Wynndel, Darcie Shepard Farm, 49°10′N, 116°32′W
12	1	AF147631 (G1)	California, Lassen Co., Likely Mountain, 5.4 mi S of Likely on Hwy. 395, 41°09′N, 120°34′W
13	1	AF147630 (G2)	California, Nevada Co., Sagehen Creek, 3 mi N Hobart Mills, 39°28′N, 120°07′W
14	1	AF147629 (I1)	California, Siskiyou Co., near Mount Hebron, 41°42′N, 121°58′W

Appendix A (*continued*)

Sample sites	*n*	Specimen ID (haplotype designation)	Locality
15	5	JMS265 (K2), JMS266 (K2), JMS267 (K2), JMS268 (K2), JMS269 (K2)	Idaho, Adams Co., Boulder Creek, 45°07′N, 116°25′W
16	4	JRD120 (M), JRD121 (M), JRD122 (M), JRD123 (M)	Idaho, Butte Co., Craters of the Moon National Monument, 20 mi SW Arco, 43°27′N, 113°33′W
17	3	JRD125 (F4), JRD126 (F4), JRD127 (F4)	Idaho, Caribou Co., 3 km N Bonneville Peak, FR13, 42°49′N, 112°06′W
18	1	UIVC10178641 (F2)	Idaho, Cassia Co., Independence Lakes, 42°11′N, 113°39′W
19	5	JRD108 (J5), JRD109 (M), JRD110 (M), JRD111 (J5), JRD112 (M)	Idaho, Custer Co., 5 km NE Ruffneck Peak, Seafoam Lakes, FR010, 44°30′N, 115°07′W
20	5	JRD128 (J1), JRD129 (J3), JRD130 (J3), JRD131 (J2), JRD132 (J3)	Idaho, Fremont Co., 10 km NE Warm River, Snow Creek, FR092, 44°08′N, 112°06′W
21	2	FMNH126101 (J2), FMNH126102 (J2)	Idaho, Idaho Co., 4–5 mi W, 2.75 mi S confluence of Lochsa and Selway Rivers, 46°06′N, 115°40′W
22	2	JRD028 (K2), JRD029 (K2)	Idaho, Idaho Co., 6 mi SW Riggins, Bald Mountain, FR571/2109 intersection, 45°22′N, 116°26′W
23	5	JRD115 (J4), JRD116 (J6), JRD117 (J7), JRD118 (J4), JRD119 (J4)	Idaho, Lemhi Co., 6 km NE Bear Mountain, FR523, 44°22′N, 113°23′W
24	5	JRD023 (C1), JMS279 (C4), JMS280 (C4), JMS281 (C4), UIVC1167 (C4)	Idaho, Nez Perce Co., 4 mi S Waha Lake, 540 Road, 46°12′N, 116°47′W
25	1	JMG008 (K1)	Idaho, Washington Co., 27 mi NW Cambridge, W slope Cuddy Mountain, E Fork Brownlee Ck., 44°47′N, 116°54′W
26	5	FMNH126103 (J2), FMNH126104 (J2), FMNH126105 (J2), FMNH126106 (J2), FMNH126107 (J2)	Montana, Granite Co., Brewster Creek, 1.1 mi N, 1.1 mi W Sliderock Mountain, 46°36′N, 113°35′W
27	5	JMS196 (L1), JMS198 (L1), JMS219 (L9), JMS220 (L10), JMS221 (L11)	Montana, Lincoln Co., 7–15 mi N of Libby, 48°24′N, 115°33′W
28	1	CMNH79-32 (J2)	Montana, Silver Bow Co., Lime Gulch Divide, 45°46′N, 112°43′W

Appendix A (*continued*)

Sample sites	*n*	Specimen ID (haplotype designation)	Locality
29	5	JRD102 (G4), JRD103 (G5), JRD104 (G3), JRD105 (G6), JRD106 (G6)	Nevada, Washoe Co., Little Valley, Whittell Forest & Wildlife Area, 4 mi NE Lake Tahoe, 3 mi W Highway 395, 39°16′N, 119°52′W
30	6	JRD077 (E7), JRD078 (E7), JRD080 (E7), JRD081 (E4), JRD082 (E3), JRD083 (E3)	Oregon, Crook Co., Ochoco Mountains, FR3550 off Route 26, Wildcat Mountain, 44°25 N, 120°32′W
31	1	CMNH81-382 (A2)	Oregon, Deschutes Co., Head of Fall Creek, SE of South Sister, 44°01′N, 121°44′W
32	4	JMG004 (E8), JMG005 (E2), JMG006 (E1), JMG007 (E2)	Oregon, Harney Co., 17 mi N Burns, Highway 396, Idlewild Campground, 43°47′N, 118°59′W
33	1	CMNH80-702 (A2)	Oregon, Hood River Co., Tilly Jane Creek, NE side of Mount Hood, 45°23′N, 121°39′W
34	3	SOU1814 (H1), SOU1874 (H1), SOU1889 (H1)	Oregon, Klamath Co., Buck Peak area, 42°16′N, 122°07′W
35	1	SOU1012 (I3)	Oregon, Lake Co., 10 mi N of Lakeview, Chandler State Park., 42°26′N, 120°19′W
36	3	SOU1011 (I2), SOU2418 (I2), SOU2369 (E8)	Oregon, Lake Co., Hart Antelope Refuge, Hot Spring Camp Area, 42°29′N, 119°41′W
37	5	JRD089 (C5), JRD090 (C6), JRD091 (C5), JRD092 (C5), JRD093 (C5)	Oregon, Wallowa Co., 22 km E Sentinel Peak, FR3925 off Route 29, 45°08′N, 117°01′W
38	5	NEOR184 (C2), NEOR185 (C2), NEOR186 (C3), NEOR187 (C2), NEOR188 (C2)	Oregon, Wallowa Co., Rye Ridge, 45°58′N, 117°10′W
39	5	JRD084 (E6), JRD085 (E6), JRD086 (E8), JRD087 (E5), JRD088 (E6)	Oregon, Wheeler Co., 12 km NE Spray, Whitetail Butte, FR 25 off Rt. 207, 44°57′N, 119°42′W
40	5	FMNH138224 (F1), FMNH138225 (F4), FMNH138228 (F3), FMNH138229 (F2), FMNH138230 (F2)	Utah, Box Elder Co., Raft River Mountains, The Meadows, Heads of George and Clear Creeks, 41°55′N, 113°24′W
41	2	UWBM41852 (B2), UWBM41854 (B2)	Washington, Chelan Co., Loop Hill, 47°48′N, 120°40′W
42	1	PSM15376 (A2)	Washington, Clallum Co., Hurricane Ridge, 47°56′N, 123°24′W

Appendix A (*continued*)

Sample sites	*n*	Specimen ID (haplotype designation)	Locality
43	4	JRD063 (D2), UWBM73663 (D1), UWBM73664 (D3), UWBM73669 (D4)	Washington, Columbia Co., 3.4 mi on FS#6437 (off FS#64), 46°07′N, 117°50′W
44	2	JRD157 (L1), JRD158 (L8)	Washington, Ferry Co., 5 km E Curlew Lake, Herron Creek Rd., 48°42′N 118°40′W
45	1	AF147632 (A2)	Washington, Kittitas Co., 2 mi S, 0.5 mi W Roslyn, Cle Elum River, 47°13′N, 120°59′W
46	5	JRD006 (A2), JRD007 (A2), JRD008 (A6), JRD009 (B2), JRD010 (A2)	Washington, Kittitas Co., N Fork of Gold Creek, 3 mi NE of Cliffdell, FR1703, 46°55′N, 121°02′W
47	3	UWBM73827 (A2), UWBM73833 (A3), UWBM73834 (A2)	Washington, Klickitat Co., Simcoe Mountain, Monument Road, 45°58′N, 120°54′W
48	3	UWBM74008 (A2), UWBM74009 (A2), UWBM74011 (A1)	Washington, Lewis Co., Mud Lake, 46°23′N, 121°36′W
49	3	UWBM73620 (L1), UWBM73626 (L1), UWBM73627 (L2)	Washington, Okanogan Co., off FS#4953 (off Hwy20), FS#50, 48°49′N, 119°02′W
50	1	JMS207 (AF401944) (L7)	Washington, Pend Oreille Co., 3.7 mi. NE Sullivan Lake, 48°50′N, 117°17′W
51	1	UWBM73983 (A2)	Washington, Pierce Co., Government Meadows, 47°05′N, 121°24′W
52	1	UWBM74003 (A2)	Washington, Skamania Co., Gifford Pinchot National Forest, 48°17′N, 121°38′W
53	1	UWBM73837 (A4)	Washington, Skamania Co., Little White Salmon River, Lusk Creek, 45°54′N, 121°39′W
54	3	CMNH82-34 (A2), CMNH82-35 (A2), CMNH82-44 (A5)	Washington, Whatcom Co., 0.35 mi SSW of Point 6215, Skyline Divide, Mount Baker, 48°51′N, 121°50′W
55	1	CMNH97-1303 (AF401781) (N)	Washington, Whitman Co., Smoot Hill Ecological Reserve, 46°49′N, 117°14′W
56	4	JRD031 (J2), JRD032 (J2), JRD033 (J2), JRD034 (J2)	Wyoming, Park Co., 8 km SE Pilot Peak, Lily Lake, FR130 off Hwy 212, 44°56′N, 109°42′W
57	1	AF147633 (F4)	Wyoming, Park Co., Yellowstone NP, Slough Creek, Scout Cabin, 44°57′N, 110°16′W
T. dorsalis	1	AF147640	Utah, Beaver Co.
T. merriami	1	AF147644	California, Riverside Co.
T. minimus	1	JRD041	Wyoming, Park Co., 4 km E Beartooth Butte, Island Lake Campground, off Hwy 212, 44°56′N, 109°32′W
T. ruficaudus	1	RBCM19683 (AF401921)	British Columbia, source of Akamina Creek, ~30 mi from Wall Lake, 49°01′N, 114°04′W
T. senex	1	JRD075 (AF40941)	Oregon, Deschutes Co., 7 km S South Sister Mountain, Sparks Lake, 44°01′N, 121°44′W
T. sibiricus	1	AF147667	Russia, Magadanskaya Oblast, Ola River
T. siskiyou	1	AF147668	Oregon, Jackson Co., Union Creek

Appendix A (*continued*)

Sample sites	*n*	Specimen ID (haplotype designation)	Locality
T. speciosus	1	JRD107	Nevada, Washoe Co., Little Valley, Whittell Forest & Wildlife Area, 4 mi NE Lake Tahoe, 3 mi W Hwy 395, 39°16′N, 119°52′W
T. townsendii	1	UWBM73649	Washington, Mason Co., 6.8 road mi from FS25 turnoff from Hwy 101, 43°35′N, 123°08′W
T. umbrinus	1	AF147677	Utah, Beaver Co.

Note. AFXXXXX - GenBank sequences, CMNH - Connor Museum of Natural History, Washington State University, FMNH - Field Museum of Natural History, JMG - Jeff M. Good field number, deposited in the University of Idaho Vertebrate Collection, JMS - Jack M. Sullivan field number, deposited in the University of Idaho Vertebrate Collection, JRD - John R. Demboski field number, deposited in the University of Idaho Vertebrate Collection, NEOR - Nez Perce Tribe, Angela Sonnedaa, PMA - Provincial Museum of Alberta, PSM - Puget Sound Museum, University of Puget Sound, RBCM - Royal British Columbia Museum, SOU-Southern Oregon University, UIVC - University of Idaho Vertebrate Collection, UWBM - University of Washington, Burke Museum.

References

Allen, J.A., 1891. A review of some of the North American ground squirrels of the genus *Tamias*. Bull. Am. Mus. Nat. Hist. III, 42–65.

Arbogast, B.S., 1999. Mitochondrial DNA phylogeography of the New World flying squirrels (*Glaucomys*): implications for Pleistocene biogeography. J. Mammal. 80, 142–155.

Arbogast, B.S., Kenagy, G.J., 2001. Comparative phylogeography as an integrative approach in biogeography, guest editorial. J. Biogeogr. 28, 819–825.

Avise, J., 2000. Phylogeography, The History and Formation of Species. Harvard University Press, Cambridge, MA.

Avise, J.C., Johns, G.C., 1999. Proposal for a standardized temporal scheme of biological classification for extant species. Proc. Natl. Acad. Sci. USA 96, 7358–7363.

Baker, R.G., 1983. Holocene vegetational history of the western United States. In: Wright, H.E. (Ed.), Late Quaternary Environments of the United States. University of Minnesota Press, Minneapolis, MN.

Bibb, M.J., Van Etten, R.A., Wright, C.T., Walberg, M.W., Clayton, D.A., 1981. Sequence and gene organization of mouse mitochondrial DNA. Cell 26, 167–180.

Blossom, P.M., 1937. Description of a race of chipmunk from south central Idaho. Occas. Pap. Museum Zool. 366, 1–3.

Brunsfeld, S.J., Sullivan, J., Soltis, D.E., Soltis, P.S., 2001. Comparative phylogeography of northwestern North America: a synthesis. In: Silvertown, J., Antonovics, J. (Eds.), Integrating Ecological and Evolutionary Processes in a Spatial Context. Blackwell Science, Oxford, pp. 319–339.

Castelloe, J., Templeton, A.R., 1994. Root probabilities for intraspecific gene trees under neutral coalescent theory. Mol. Phylogenet. Evol. 3, 102–113.

Clement, M., Posada, D., Crandall, K.A., 2000. TCS: a computer program to estimate gene genealogies. Mol. Ecol. 9, 1657–1659.

Conroy, C.J., Cook, J.A., 2000. Phylogeography of a post-glacial colonizer: *Microtus longicaudus* (Rodentia: Muridae). Mol. Ecol. 9, 165–175.

Cook, J.A., Bidlack, A.L., Conroy, C.J., Demboski, J.R., Fleming, M.A., Runck, A.M., Stone, K.D., MacDonald, S.O., 2001. A phylogeographic perspective on endemism in the Alexander Archipelago of southeast Alaska. Biol. Conserv. 97, 215–227.

Cook, J.A., MacDonald, S.O., 2001. Should endemism be a focus of conservation efforts along the North Pacific Coast of North America. Biol. Conserv. 97, 201–213.

Dalquest, W.W., 1948. Mammals of Washington. University of Kansas Publications, Museum of Natural History, Lawrence, KS.

Daubenmire, R., 1975. Floristic plant geography of eastern Washington and Northern Idaho. J. Biogeogr. 2, 1–18.

Debry, R.W., Olmstead, R.G., 2000. A simulation study of reduced tree-search effort in bootstrap resampling analysis. Syst. Biol. 49, 171–179.

Delcourt, P.A., Delcourt, H.R., 1993. Paleoclimates, paleovegetation, and paleofloras during the Late Quaternary. In: Flora North America. Oxford University Press, New York, pp. 71–94.

Demboski, J.R., Cook, J.A., 2001. Phylogeography of the dusky shrew, *Sorex monticolus* (Insectivora, Soricidae): insight into deep and shallow history in northwestern North America. Mol. Ecol. 10, 1227–1240.

Demboski, J.R., Stone, K.D., Cook, J.A., 1999. Further perspectives on the Haida Gwaii glacial refugium. Evolution 53, 2008–2012.

Ellis, L.S., Maxson, L.R., 1979. Evolution of the chipmunk genera *Eutamias* and *Tamias*. J. Mammal. 60, 331–334.

Felsenstein, J., 1985. Confidence limits on phylogenies: an approach using the bootstrap. Evolution 39, 783–791.

Felsenstein, J., 1988. Phylogenies from molecular sequences: inference and reliability. Annu. Rev. Genet. 22, 521–565.

Gill, F.B., Mostrom, A.M., Mack, A.L., 1993. Speciation in North American chickadees: I. Patterns of mtDNA genetic divergence. Evolution 47, 195–212.

Goldman, N., 1993. Statistical tests of models of DNA substitution. J. Mol. Evol. 36, 182–198.

Good, J.M., Sullivan, J., 2001. Phylogeography and species limits of red-tailed chipmunks (*Tamias ruficaudus*), a Northern Rocky Mountain endemic. Mol. Ecol. 10, 2683–2695.

Good, J.M., Demboski, J.R., Nagorsen, D.W., Sullivan, J.M., in press. Phylogeography and introgressive hybridization: chipmunks (*Tamias*) in the Northern Rocky Mountains. Evolution.

Graham, A., 1999. Late Cretaceous and Cenozoic History of North American Vegetation. Oxford University Press, New York.

Gu, X., Fu, Y.-X., Li, W.-H., 1995. Maximum likelihood estimation of the heterogeneity of substitution rate among nucleotide sites. Mol. Biol. Evol. 12, 546–557.

Gustincich, S., Manfioletti, G., Del Sal, G., Schneider, C., Carnichi, P., 1991. A fast method for high quality genomic DNA extraction from whole human blood. Biotechniques 11, 298–301.

Hadley, E.A., 1996. Influence of Late-Holocene climate on Northern Rocky Mountain mammals. Quat. Res. 46, 298–310.

Hall, E.R., 1981. The Mammals of North America, second ed. Wiley, New York.

Harris, D.J., Rogers, D.S., Sullivan, J., 2000. Phylogeography of *Peromyscus furvus* (Rodentia; Muridae) based on cytochrome *b* sequence data. Mol. Ecol. 9, 2129–2135.

Hasegawa, M., Kishino, M., Yano, T., 1985. Dating the human-ape split by a molecular clock of mitochondrial DNA. J. Mol. Evol. 22, 160–174.

Hewitt, G.M., 1996. Some genetic consequences of ice ages, and their role in divergence and speciation. Biol. J. Linn. Soc. 58, 247–276.

Hoffmann, R.S., 1981. Different voles for different holes: environmental restrictions on refugial survival of mammals. In: Proceedings of the Second International Congress of Systematic and Evolutionary Biology, Vancouver, British Columbia, pp. 25–45.

Hoffmann, R.S., Anderson, C.G., Thorington, R.J., Heaney, L., 1993. Family Sciuridae. In: Wilson, D.E., Reeder, D.M. (Eds.), Mammal Species of the World: A Taxonomic and Geographic Reference. Smithsonian Institution Press, Washington, pp. 419–465.

Howell, A.H., 1929. Revision of the American Chipmunks, U.S. Department of Agriculture, Bureau of Biological Survey, Washington, DC, No. 52.

Irwin, D.M., Kocher, T.D., Wilson, A.C., 1991. Evolution of the cytochrome *b* gene of mammals. J. Mol. Evol. 32, 128–144.

Jameson, E.W.J., 1999. Host–ectoparasite relationships among North America chipmunks. Acta Ther. 44, 225–231.

Johnson, D.H., 1943. Systematic review of the chipmunks (genus *Eutamias*) of California. Univ. Calif. Publ. Zool. 48, 63–148.

Johnson, P.J., 1987. Larval taxonomy, biology, and biogeography of the genera of North American Byrrhidae. M.S. Thesis. University of Idaho, Moscow, ID.

Jukes, T.H., Cantor, C.R., 1969. Evolution of protein molecules. In: Munro, H.N. (Ed.), Mammalian Protein Metabolism. Academic Press, New York, pp. 21–132.

Kimura, M., 1980. A simple method for estimating evolutionary rate of base substitution through comparative studies of nucleotide sequences. J. Mol. Evol. 10, 111–120.

Lanavé, C., Preparata, G., Saccone, C., Serio, G., 1984. A new method for calculating evolutionary substitution rates. J. Mol. Evol. 20, 86–93.

Levenson, H., Hoffmann, R.S., Nadler, C.F., Deutsch, L., Freeman, S.D., 1985. Systematics of the Holarctic chipmunks (*Tamias*). J. Mammal. 66, 219–242.

Merriam, C.H., 1903. Eight new mammals from the United States. Proc. Biol. Soc. Wash. 16, 73–78.

Nadler, C.F., Hoffmann, R.S., Honacki, J.H., Pozin, D., 1977. Chromosomal evolution in chipmunks, with special emphasis on A and B karyotypes of the subgenus *Neotamias*. Am. Mid. Nat. 98, 343–353.

Nielson, M., Lohman, K., Sullivan, J., 2001. Phylogeography of the tailed frog (*Ascaphus truei*): implications for the biogeography of the Pacific Northwest. Evolution 55, 147–160.

Piaggio, A.J., Spicer, G.S., 2000. Molecular phylogeny of the chipmunk genus *Tamias* based on the mitochondrial cytochrome oxidase subunit II gene. J. Mammal Evol. 7, 147–156.

Piaggio, A.J., Spicer, G.S., 2001. Molecular phylogeny of the chipmunks inferred from mitochondrial cytochrome *b* and cytochrome oxidase II gene sequences. Mol. Phylogenet. Evol. 20, 335–350.

Posada, D., Crandall, K.A., 2001. Inraspecific gene genealogies: trees grafting into networks. TREE 16, 37–45.

Posada, D., Crandall, K.A., Templeton, A.R., 2000. GeoDis: a program for the cladistic nested analysis of the geographical distribution of genetic haplotypes. Mol. Ecol. 9, 487–488.

Riddle, B.R., 1996. The molecular phylogeographic bridge between deep and shallow history in continental biotas. TREE 11, 207–212.

Riddle, B.R., Hafner, D.J., 1999. Species as units of analysis in ecology and biogeography: time to take the blinders off. Global Ecol. Biogeogr. 8, 433–441.

Smith, M.F., Thomas, W.K., Patton, J.L., 1992. Mitochondrial DNA-like sequence in the nuclear genome of an akodontine rodent. Mol. Biol. Evol. 9, 204–215.

Soltis, D.E., Gitzendanner, M.A., Strenge, D.D., Soltis, P.E., 1997. Chloroplast DNA intraspecific phylogeography of plants from the Pacific Northwest of North America. Plant Syst. Evol. 206, 353–373.

Steppan, S.J., Akhverdyan, M.R., Lyapunova, E.A., Fraser, D.G., Voronstov, N.N., Hoffmann, R.S., Braun, M.J., 1999. Molecular phylogeny of the Marmots (Rodentia: Sciuridae): tests of evolutionary and biogeographic hypotheses. Syst. Biol. 48, 715–734.

Sullivan, J., Markert, J., Kilpatrick, C.W., 1997. Phylogeography and molecular systematics of the *Peromyscus aztecus* species group (Rodentia: Muridae) inferred using parsimony and likelihood. Syst. Biol. 46, 426–440.

Sullivan, J., Arellano, E.A., Rogers, D.S., 2000. Comparative phylogeography of Mesoamerican highland rodents: Concerted versus independent responses to past climatic fluctuations. Am. Nat. 155, 755–768.

Sutton, D.A., 1982. The female genital bone of chipmunks, genus *Eutamias*. Southwest. Nat. 27, 393–402.

Sutton, D.A., 1992. *Tamias amoenus*. In: Hood, C.S. (Ed.), Mammalian Species. The American Society of Mammalogists.

Swofford, D.L., 2001. PAUP*: Phylogenetic Analysis Using Parsimony (*and Other Methods). ver. 4.0. Sinauer Associates, Sunderland, MA.

Templeton, A.R., 1998. Nested clade analyses of phylogeographic data: testing hypotheses about gene flow and population history. Mol. Ecol. 7, 381–397.

Templeton, A.R., Boerwinkle, E., Sing, C.F., 1987. A cladistic analysis of phenotypic associations with haplotypes inferred from restriction endonuclease mapping. I. Basic theory and an analysis of alcohol dehydrogenase activity in *Drosophila*. Genetics 117, 343–351.

Templeton, A.R., Crandall, K.A., Sing, C.F., 1992. A cladistic analysis of phenotypic associations with haplotypes inferred from restriction endonuclease mapping and DNA sequence data. III. Cladogram estimation. Genetics 132, 619–633.

Templeton, A.R., Routman, E., Phillips, C.A., 1995. Separating population structure from population history: a cladistic analysis of the geographical distribution of mitochondrial DNA haplotypes in the tiger salamander, *Ambystoma tigrinum*. Genetics 140, 767–782.

Templeton, A.R., Sing, C.F., 1993. A cladistic analysis of phenotypic associations with haplotypes inferred from restriction endonuclease mapping. IV. Nested analyses with cladogram uncertainty and recombination. Genetics 134, 659–669.

Verts, B.J., Carraway, L.N., 1998. Land Mammals of Oregon. University of California, Berkeley.

Webb, T.I., Bartlein, P.J., 1992. Global changes during the last 3 million years: climatic controls and biotic responses. Annu. Rev. Ecol. Syst. 23, 141–173.

White, J.A., 1953. The baculum in the chipmunks of western North America. Univ. Kansas Publ. Mus. Nat. Hist. 5 (35), 611–631.

Wolfe, J.A., 1978. A paleobotanical interpretation of the Tertiary climates in the Northern Hemisphere. Am. Scientist 66, 694–703.

Wooding, S., Ward, R., 1997. Phylogeography and Pleistocene evolution in the North American black bear. Mol. Biol. Evol. 14, 1096–1105.

Yang, Z., 1994. Maximum likelihood phylogenetic estimation from DNA sequences with variable rates over sites; approximate methods. J. Mol. Evol. 39, 306–314.

Yang, Z., Goldman, N., Friday, A., 1995. Maximum likelihood trees from DNA sequences: a peculiar statistical estimation problem. Syst. Biol. 44, 384–399.

Zink, R.M., 1996. Comparative phylogeography in North American birds. Evolution 50, 308–317.